

# Azimuthal spin asymmetries in pion-polarized proton induced Drell-Yan process at COMPASS using holographic light-front QCD

Bheemsehan Gurjar<sup>a</sup>, Chandan Mondal<sup>b,c,d</sup>

<sup>a</sup>*Indian Institute of Technology Kanpur, Kanpur-208016, India*

<sup>b</sup>*Institute of Modern Physics, Chinese Academy of Sciences, Lanzhou, Gansu, 730000, China*

<sup>c</sup>*School of Nuclear Physics, University of Chinese Academy of Sciences, Beijing, 100049, China*

<sup>d</sup>*CAS Key Laboratory of High Precision Nuclear Spectroscopy, Institute of Modern Physics, Chinese Academy of Sciences, Lanzhou 730000, China*

## Abstract

We compute all the leading-twist azimuthal spin asymmetries in the pion-proton induced Drell-Yan process. These spin asymmetries arise from convolutions of the leading-twist transverse-momentum-dependent parton distributions (TMDs) of both the incoming pion and the target proton. We employ the holographic light-front pion wave functions for the pion TMDs, while for the proton TMDs, we utilize a light-front quark-diquark model constructed by the soft-wall AdS/QCD. The gluon rescattering is crucial to predict nonzero time-reversal odd TMDs. We study the utility of a nonperturbative SU(3) gluon rescattering kernel, which extends beyond the typical assumption of perturbative U(1) gluons. Subsequently, we employ Collins-Soper scale evolution at Next-to-Leading Logarithmic precision for the TMDs evolution. Our predictions for the spin asymmetries are consistent with the available experimental data from COMPASS and other phenomenological studies.

*Keywords:* Single Spin Asymmetries, Drell-Yan process, TMDs, Light-front holography

## 1. Introduction

Over the last two decades, studying dilepton production in high-energy hadron-hadron collisions, known as the Drell-Yan (DY) process [1, 2], has emerged as a crucial method for gaining insights into the fundamental structure of hadrons, notably through the analysis of parton distributions. The differential cross-section of the DY process follows the transverse momentum-dependent factorization at small photon transverse momentum  $q_\perp$ , i.e.,  $q_\perp \ll Q$ , where  $Q$  defines the hard scale, representing the invariant mass of the dilepton pair. This factorization entails convolving perturbatively calculable hard-scattering partonic cross sections with transverse momentum-dependent parton distributions (TMDs) [3–5]. The TMDs are crucial for understanding spin and transverse momentum correlations, as well as the three-dimensional structure of hadrons in the momentum space. They are accessible in semi-inclusive deep inelastic scattering (SIDIS) [6–8] and DY processes [9–12].

The Sivers function [13] characterizes the asymmetric distribution of unpolarized quarks within a transversely polarized nucleon, establishing a correlation between the quark's transverse momentum and the nucleon's trans-

verse spin. Due to its time-reversal odd (T-odd) property, the sign of the Sivers function measured in the DY process is expected to be opposite to its sign measured in SIDIS [14]. In the last decade, HERMES [15, 16], COMPASS [17–20], and Jlab Hall A [21] Collaborations have extensively investigated the Sivers asymmetry in SIDIS. Confirming the observed sign change is a crucial test for our understanding of QCD dynamics and the factorization scheme [14, 22–26]. This validation not only serves as a fundamental assessment but also remains a central focus on current and future DY facilities [27–30]. In the pion-polarized proton DY process, the convolution of the pion's unpolarized TMD and the proton's Sivers functions generates a  $\sin(\phi_s)$  modulated azimuthal asymmetry [12].

Another leading twist T-odd proton distribution function, known as the Boer-Mulders function, describes the distribution of transversely polarized quarks within an unpolarized proton. It originates from the correlation between the transverse spin and transverse momentum of the quark [10, 31]. In the pion-proton induced DY process, the convolution of the pion's and the proton's Boer-Mulder functions result in a  $\cos(2\phi)$  azimuthal angular dependence of the final-state dilepton. The proton's Boer-Mulders function has been extensively studied using QCD-inspired models [32–42]. While the pion's Boer-Mulders function remains unexplored experimentally, various phenomenological models have been employed to calculate this

*Email addresses:* gbeem@iitk.ac.in (Bheemsehan Gurjar), mondal@impcas.ac.cn (Chandan Mondal)

distribution [43–50].

The Kotzinian-Mulders function and pretezelosity distribution, denoted as  $h_{1L}^\perp$  and  $h_{1T}^\perp$ , respectively describe the probability of finding a transversely polarized quark within a longitudinally and transversely polarized nucleon, respectively. Like the Boer-Mulders function, they are also chiral-odd distributions. In the pion-proton induced DY process, they combine with the pion Boer-Mulders function, leading to the  $\sin(2\phi_s)$  and  $\sin(2\phi + \phi_s)$  modulated azimuthal spin asymmetry, respectively [12, 51].

In this work, we calculate four azimuthal spin asymmetries in the pion-polarized proton induced DY process: Sivers ( $\sin(\phi_s)$ ),  $\sin(2\phi + \phi_s)$ , Boer-Mulders ( $\cos(2\phi)$ ), and  $\sin(2\phi_s)$  asymmetries, within the framework of TMD factorization [52]. We utilize the leading-twist pion TMDs obtained using light-front holographic pion wave functions [47] and the proton TMDs calculated in a light-front quark-diquark model constructed by the soft-wall AdS/QCD [38, 53]. We employ both the perturbative U(1) and the non-perturbative SU(3) gluon rescattering kernels to obtain the T-odd pion and proton TMDs. We then apply QCD evolution of the TMDs in order to incorporate degrees of freedom relevant to higher-resolution probes [54]. This then allows us to compare our QCD-evolved TMDs leading to the azimuthal spin asymmetries with experimental data from COMPASS Collaboration [27, 28] and various phenomenological studies [12].

## 2. DY process with pion and polarized proton

The pion-induced Drell-Yan process can be described as [55]

$$\pi^-(P_\pi) + p^\uparrow(P_p) \rightarrow \gamma^*(q_\perp) + X \rightarrow l^+(\ell) + l^-(\ell') + X \quad (1)$$

where  $P_\pi$  and  $P_p$  denote the four-momenta of the incoming pion beam and the proton target, while  $q_\perp$  represents the transverse momenta of the intermediate virtual photon. The momenta of the outgoing dilepton pair are designated by  $\ell$  and  $\ell'$ . The differential cross section for the  $\pi$ -p Drell-Yan process with a transversely polarized target is expressed by the following generic form [29, 55]

$$\begin{aligned} \frac{d\sigma}{d^4 q d\Omega} = & \frac{\alpha_{\text{em}}^2}{\mathcal{F} Q^2} \left\{ \left[ (1 + \cos^2 \theta) F_{UU}^1 + \sin^2 \theta \cos(2\phi) F_{UU}^{\cos 2\phi} \right] \right. \\ & + S_L \sin^2 \theta \sin(2\phi) F_{UL}^{\sin 2\phi} + S_T (1 - \cos^2 \theta) \sin \phi_S F_{UT}^{\sin \phi_S} \\ & + S_T \sin^2 \theta [\sin(2\phi + \phi_S) F_{UT}^{\sin(2\phi + \phi_S)} \\ & \left. + \sin(2\phi - \phi_S) F_{UT}^{\sin(2\phi - \phi_S)} \right] \} \end{aligned} \quad (2)$$

In the above Eq. (2), the azimuthal angle of the target polarization vector  $S_T$  is represented as  $\phi_S$ , while in the Collins-Soper frame [56], the azimuthal and polar angles of the lepton momentum are denoted by  $\phi$  and  $\theta$ , respectively.  $\mathcal{F}$  is the flux factor of the incoming hadrons.  $\Omega$  is

the solid angle of the dilepton system. The first subscript on the structure functions  $F_{XY}$  indicates that the pion is unpolarized ( $U$ ), while the second subscript corresponds to the proton polarization, which can be either unpolarized ( $U$ ), longitudinally ( $L$ ), or transversely ( $T$ ) polarized.

The single spin asymmetry is obtained by taking the ratio of polarized structure functions to unpolarized structure functions [4, 12],

$$A_{XY}^{\text{weight}}(x_\pi, x_p, q_\perp, Q^2) = \frac{F_{XY}^{\text{weight}}(x_\pi, x_p, q_\perp, Q^2)}{F_{UU}^1(x_\pi, x_p, q_\perp, Q^2)}. \quad (3)$$

Note that all the structure functions and asymmetries depend on the Bjorken variables  $x_\pi$  and  $x_p$  for the pion and proton, respectively, as well as the transverse momentum  $q_\perp$  and virtuality  $Q^2$  of the photon. Those structure functions can be expressed as the convolution of the TMDs of the pion and proton [55],

$$\begin{aligned} F_{UU}^1 &= \mathcal{C} [f_{1,\pi} f_{1,p}], \\ F_{UU}^{\cos(2\phi)} &= \mathcal{C} \left[ \frac{2(\hat{h} \cdot \vec{p}_{\perp\pi})(\hat{h} \cdot \vec{p}_{\perp p}) - \vec{p}_{\perp\pi} \cdot \vec{p}_{\perp p} h_{1,\pi}^\perp h_{1,p}^\perp}{M_\pi M_p} \right], \\ F_{UL}^{\sin(2\phi)} &= -\mathcal{C} \left[ \frac{2(\hat{h} \cdot \vec{p}_{\perp\pi})(\hat{h} \cdot \vec{p}_{\perp p}) - \vec{p}_{\perp\pi} \cdot \vec{p}_{\perp p} h_{1,\pi}^\perp h_{1L,p}^\perp}{M_\pi M_p} \right], \\ F_{UT}^{\sin(\phi_S)} &= \mathcal{C} \left[ \frac{\hat{h} \cdot \vec{p}_{\perp p} f_{1,\pi} f_{1T,p}^\perp}{M_p} \right], \\ F_{UT}^{\sin(2\phi - \phi_S)} &= -\mathcal{C} \left[ \frac{\hat{h} \cdot \vec{p}_{\perp\pi} h_{1,\pi}^\perp h_{1,p}}{M_\pi} \right], \\ F_{UT}^{\sin(2\phi + \phi_S)} &= -\mathcal{C} \left[ \left\{ \frac{2(\hat{h} \cdot \vec{p}_{\perp p})[2(\hat{h} \cdot \vec{p}_{\perp\pi})(\hat{h} \cdot \vec{p}_{\perp p}) - \vec{p}_{\perp\pi} \cdot \vec{p}_{\perp p}]}{2M_\pi M_p^2} \right. \right. \\ & \left. \left. - \frac{p_{\perp p}^2 (\hat{h} \cdot \vec{p}_{\perp\pi})}{2M_\pi M_p^2} \right\} h_{1,\pi}^\perp h_{1T,p}^\perp \right], \end{aligned} \quad (4)$$

where  $\mathcal{C}$  stands for the convolution integrals,  $\hat{h} = \vec{q}_\perp / |q_\perp|$  is a unit vector pointing out along the  $x$ -axis in the Collins-Soper frame. The convolution integral mentioned above is defined as [55],

$$\mathcal{C} [\omega f_\pi f_p] = \sum_i e_i^2 \int d^2 \vec{p}_{\perp\pi} d^2 \vec{p}_{\perp p} \delta^{(2)}(\vec{q}_\perp - \vec{p}_{\perp\pi} - \vec{p}_{\perp p}) \times \omega(\vec{q}_\perp, \vec{p}_{\perp\pi}, \vec{p}_{\perp p}) f_{i,p}(x_p, \vec{p}_{\perp p}) f_{\bar{i},\pi}(x_\pi, \vec{p}_{\perp\pi}), \quad (5)$$

where the sum runs for all active quark flavors  $i = u, \bar{u}, d, \bar{d}, \dots$ , and  $\omega$  is a kinetic weight function, which projects out the corresponding azimuthal angular dependence. The convolution variables  $\vec{p}_{\perp\pi}$ ,  $\vec{p}_{\perp p}$  correspond to the relative transverse momenta of struck quarks in the pion and proton, respectively.

## 3. QCD evolution of structure functions

To compare the model results for spin asymmetries with available experimental data, it is necessary to evolve the

structure functions. Following the TMD factorization theorem, these structure functions can be evolved from an initial model scale,  $Q_0^{p/\pi}$ , to a higher relevant scale,  $Q$ , using the Collins-Soper-Sterman (CSS) evolution framework [3, 52, 57]. The CSS evolution of structure functions can be performed in impact parameter space. All the evolved structure functions can be represented in terms of impact parameter-dependent TMDs and Sudakov form factors as follows [4, 58],

$$\begin{aligned} F_{UU}^1(x_\pi, x_p, q_\perp, Q^2) &= \mathcal{B}_0 \left[ \tilde{f}_{1,\pi} \tilde{f}_{1,p} \right], \\ F_{UU}^{\cos(2\phi)}(x_\pi, x_p, q_\perp, Q^2) &= M_\pi M_p \mathcal{B}_2 \left[ \tilde{h}_{1,\pi}^{\perp(1)} \tilde{h}_{1,p}^{\perp(1)} \right], \\ F_{UL}^{\sin(2\phi)}(x_\pi, x_p, q_\perp, Q^2) &= -M_\pi M_p \mathcal{B}_2 \left[ \tilde{h}_{1,\pi}^{\perp(1)} \tilde{h}_{1L,p}^{\perp(1)} \right], \\ F_{UT}^{\sin(\phi_s)}(x_\pi, x_p, q_\perp, Q^2) &= M_p \mathcal{B}_1 \left[ \tilde{f}_{1,\pi} \tilde{f}_{1T,p}^{\perp(1)} \right], \\ F_{UT}^{\sin(2\phi-\phi_s)}(x_\pi, x_p, q_\perp, Q^2) &= -M_\pi \mathcal{B}_1 \left[ \tilde{h}_{1,\pi}^{\perp(1)} \tilde{h}_{1,p} \right], \\ F_{UT}^{\sin(2\phi+\phi_s)}(x_\pi, x_p, q_\perp, Q^2) &= -\frac{M_\pi M_p^2}{4} \mathcal{B}_3 \left[ \tilde{h}_{1,\pi}^{\perp(1)} \tilde{h}_{1T,p}^{\perp(2)} \right], \end{aligned} \quad (6)$$

where  $\mathcal{B}_n$  is expressed as,

$$\begin{aligned} \mathcal{B}_n \left[ \tilde{F}_\pi \tilde{F}_p \right] &= \frac{1}{N_c} \sum_i e_i^2 \int \frac{b_\perp db_\perp}{2\pi} b_\perp^n J_n(q_\perp b_\perp) \\ &\times \tilde{F}_\pi^i(x_\pi, b_\perp, Q_0^\pi) \tilde{F}_p^i(x_p, b_\perp, Q_0^p) e^{-S(b_\perp, Q_0^\pi, Q_0^p, Q)}, \end{aligned} \quad (7)$$

with  $N_c$  being the number of active flavors in a particular hadron and  $J_n$  is the Bessel function of  $n$ -th order. The functions  $\tilde{F}_\pi^i$  and  $\tilde{F}_p^i$  corresponds to the pion and proton TMDs, respectively, in the impact-parameter space, obtained by performing Fourier transformation of the TMDs in momentum space at their initial model scales  $Q_0^\pi$  and  $Q_0^p$ . The impact-parameter  $b_\perp$  is the Fourier conjugate variable to  $p_{\perp h}$ , where index  $h = \pi$  or  $p$  refers to pion or proton. The Sudakov form factor,  $S(b_\perp, Q_0^\pi, Q_0^p, Q)$ , which contains the important effects of gluon radiation, is decomposed into perturbative and nonperturbative parts,

$$\begin{aligned} S(b_\perp, Q_0^\pi, Q_0^p, Q) &= 2S_{\text{pert}}(b_*, Q) + S_{\text{NP}}^p(b_\perp, Q_0^p, Q) \\ &+ S_{\text{NP}}^\pi(b_\perp, Q_0^\pi, Q). \end{aligned} \quad (8)$$

The perturbative part is given by [3],

$$S_{\text{pert}} = \int_{Q_i}^Q \frac{d\bar{\mu}}{\bar{\mu}} \left[ A(\alpha_s(\bar{\mu})) \ln \frac{Q^2}{\bar{\mu}^2} + B(\alpha_s(\bar{\mu})) \right], \quad (9)$$

where  $Q_i = 2e^{-\gamma_E}/b_*$  (with  $\gamma_E \simeq 0.577$ ), with the choice of  $b_*$  in such a way that  $b_*(b_\perp) = b_\perp/(1 + \frac{b_\perp^2}{b_{\max}^2})^{1/2} \simeq b_{\max}$  at  $b_\perp \rightarrow \infty$  and  $b_*(b_\perp) \simeq b_\perp$  when  $b_\perp \rightarrow 0$  [54]. These allow avoiding the Landau pole by freezing the scale  $b_\perp$  [52].  $b_{\max}$  separates the perturbative and nonperturbative domains of the TMDs and it is determined phenomenologically as  $b_{\max} = 1.5 \text{ GeV}^{-1}$  [59]. The above perturbative Sudakov Form factor is spin-independent and has the same form for all kind of distribution functions. The coefficients

$A$  and  $B$  in Eq. (9) are the anomalous dimensions and can be expanded perturbatively [3, 60, 61].

On the other hand, the nonperturbative proton and pion Sudakov form factors,  $S_{\text{NP}}^{p/\pi}$ , have been studied phenomenologically. A generic form for  $S_{\text{NP}}$  proposed in Ref. [52] is given by,

$$S_{\text{NP}}^{p/\pi}(b_\perp, Q_0^{p/\pi}, Q) = g_1^{p/\pi}(b_\perp) + g_2^{p/\pi}(b_\perp) \ln \frac{Q}{Q_0^{p/\pi}}, \quad (10)$$

where  $g_1^{p/\pi}(b_\perp)$  and  $g_2^{p/\pi}(b_\perp)$  depend on the hadronic distribution functions. For the proton, they read as

$$g_1^p(b_\perp) = \frac{g_1^p}{2} b_\perp^2, \quad g_2^p(b_\perp) = \frac{g_2^p}{2} \ln \frac{b_\perp}{b_*} \quad (11)$$

with  $g_1^p = 0.212 \text{ GeV}^2$  and  $g_2^p = 0.84 \text{ GeV}^2$  [62, 63], whereas for the pion, they are given by,

$$g_1^\pi(b_\perp) = g_1^\pi b_\perp^2, \quad g_2^\pi(b_\perp) = g_2^\pi \ln \frac{b_\perp}{b_*}. \quad (12)$$

The numerical values of  $g_1^\pi$  and  $g_2^\pi$  are obtained by fitting to the  $\pi^- N$  DY data [64]:  $g_1^\pi = 0.082 \text{ GeV}^2$  and  $g_2^\pi = 0.394 \text{ GeV}^2$ . By employing Eqs. (6) and (7), the QCD evolution of both unpolarized and polarized structure functions can be performed from the initial hadronic model scale  $Q_0^{p/\pi}$  to the crucial final scale  $Q$ .

## 4. Model inputs for the pion and proton TMDs

### 4.1. Pion TMDs

We employ the holographic light-front pion wave functions for the pion TMDs [65]. For the pion, there exist two leading-twist TMDs: the unpolarized quark TMD,  $f_{1,\pi}^q(x, k_\perp^2)$ , and the Boer-Mulders function,  $h_{1,\pi}^{\perp q}(x, k_\perp^2)$ . The unpolarized TMD in terms of the light-front wave functions (LFWFs) can be expressed as

$$f_{1,\pi}^q(x, k_\perp^2) = \frac{1}{16\pi^3} \sum_{h,\bar{h}} |\Psi_{h\bar{h}}(x, \vec{k}_\perp)|^2, \quad (13)$$

where  $\Psi_{h\bar{h}}(x, \vec{k}_\perp)$  represents the pion's LFWF with  $h(\bar{h})$  being the helicity of the quark (antiquark) in the leading Fock sector. The normalization condition for the unpolarized TMD is as follows:

$$\int dx d^2 \vec{k}_\perp f_{1,\pi}^q(x, k_\perp^2) = 1. \quad (14)$$

To obtain the nonzero pion Boer-Mulders function  $h_{1,\pi}^{\perp q}(x, k_\perp^2)$ , it is necessary to account for the gauge link. This represents the initial or final-state interactions of the active parton with the target remnant, collectively referred

to as the gluon rescattering kernel. The pion Boer-Mulders function can be represented as follows [47]:

$$k_\perp^2 h_{1,\pi}^{\perp q}(x, k_\perp^2) = M_\pi \int \frac{d^2 \vec{k}'_\perp}{16\pi^3} iG(x, |\vec{k}_\perp - \vec{k}'_\perp|) \times \sum_{h,\bar{h}} \Psi_{h,\bar{h}}^*(x, \vec{k}'_\perp) h k_\perp e^{ih\theta_{k_\perp}} \Psi_{h,\bar{h}}(x, \vec{k}_\perp), \quad (15)$$

where  $G(x, |\vec{k}_\perp - \vec{k}'_\perp|)$  corresponds to the gluon rescattering kernel with  $(\vec{k}_\perp - \vec{k}'_\perp)$  being the transverse momentum carried by the exchanged gluon.  $\theta_{k_\perp}$  is the polar angle in a two-dimensional polar coordinate system, ranging from 0 to  $2\pi$ . To proceed further, we must specify the form of the gluon rescattering kernel. A straightforward approach is to assume the perturbative Abelian gluon rescattering kernel, as defined by [36, 45],

$$iG^{\text{pert.}}(x, |\vec{k}_\perp - \vec{k}'_\perp|) = \frac{C_F \alpha_s}{2\pi} \frac{1}{(|\vec{k}_\perp - \vec{k}'_\perp|)^2}, \quad (16)$$

with the color factor  $C_F = 4/3$  and  $\alpha_s$  being the fixed coupling constant. An exact computation of the nonperturbative gluon rescattering kernel is currently unavailable. In practice, an approximation scheme is necessary. Meanwhile, the gluon rescattering kernel can be expressed in terms of the QCD lensing function  $I(x, |\vec{k}_\perp - \vec{k}'_\perp|)$ , as described in Ref. [47],

$$iG(x, |\vec{k}_\perp - \vec{k}'_\perp|) = -\frac{2}{(2\pi)^2} \frac{(1-x)I(x, |\vec{k}_\perp - \vec{k}'_\perp|)}{(|\vec{k}_\perp - \vec{k}'_\perp|)}. \quad (17)$$

The above relation originates from the connection between the chiral-odd GPD and the first moment of the pion Boer-Mulders function [35]. Gamberg and Schlegel deduced the QCD lensing function  $I(x, |\vec{k}_\perp - \vec{k}'_\perp|)$  from the eikonal amplitude for final-state rescattering through the exchange of non-Abelian SU(3) soft gluons [43]. The nonperturbative gluon rescattering kernel, Eq. (17), has been effectively used to calculate T-odd TMDs for both the pion [47, 48] and the proton [38].

To compute the pion's TMDs, we utilize the spin-improved holographic wave function [47, 66],

$$\Psi_{h,\bar{h}}(x, \vec{k}_\perp) = \left[ (M_\pi x(1-x) + Bm_q)h\delta_{h,-\bar{h}} - Bk_\perp e^{-ih\theta_{k_\perp}}\delta_{h,\bar{h}} \right] \frac{\Psi(x, \vec{k}_\perp)}{x(1-x)}. \quad (18)$$

where

$$\Psi(x, \vec{k}_\perp) = \mathcal{N} \frac{1}{\sqrt{x(1-x)}} \exp \left[ -\frac{k_\perp^2 + m_q^2}{2\kappa^2 x(1-x)} \right], \quad (19)$$

with  $m_q$  being the effective quark mass and  $\mathcal{N}$  is a normalization constant determined using

$$\sum_{h,\bar{h}} \int dx \frac{d^2 \vec{k}_\perp}{16\pi^3} |\Psi_{h,\bar{h}}(x, \vec{k}_\perp)|^2 = 1. \quad (20)$$

The parameter  $B$  in Eq. (18) is known as the dynamical spin parameter. When  $B \rightarrow 0$ , it signifies no spin-orbit correlations, akin to the original holographic wave function [65]. Conversely, when  $B \geq 1$ , it indicates maximal spin-orbit correlation.

With  $B \geq 1$ , the constituent quark mass  $m_q = 330$  MeV [47], and AdS/QCD scale parameter  $\kappa = 523 \pm 24$  MeV determined by simultaneous fit to the Regge slopes of mesons and baryons [67], the pion wave function has been effectively utilized to calculate various pion observables, including electromagnetic form factors, associated radii, transition form factor, parton distribution function (PDF), TMDs, etc., with notable overall success [47, 66, 68–70].

Using the pion wave function provided in Eq. (18), the explicit expression for the unpolarized quark TMD is given as follows:

$$f_{1,\pi}^q(x, k_\perp^2) = \frac{2\mathcal{N}^2}{16\pi^3} \frac{(M_\pi x(1-x) + Bm_q)^2 + B^2 k_\perp^2}{(x(1-x))^3} \times \exp \left[ -\frac{k_\perp^2 + m_q^2}{x(1-x)\kappa^2} \right]. \quad (21)$$

Using the perturbative gluon rescattering kernel given in Eq. (16), we derive an analytical expression for the pion Boer-Mulders function as follows:

$$h_{1,\pi}^{\perp q}(x, k_\perp^2) = \alpha_s B C_F \frac{M_\pi \mathcal{N}^2}{4\pi^3} \frac{M_\pi x(1-x) + Bm_q}{(x(1-x))^2} \left( \frac{\kappa}{k_\perp} \right)^2 \times \exp \left[ -\frac{k_\perp^2 + 2m_q^2}{2\kappa^2 x(1-x)} \right] \left( 1 - \exp \left[ -\frac{k_\perp^2}{2\kappa^2 x(1-x)} \right] \right). \quad (22)$$

If  $B \rightarrow 0$ , the holographic Boer-Mulders function becomes zero. However, for  $B \geq 1$ , it is hardly affected by the parameter  $B$ , as the normalization constant  $\mathcal{N}$  of the wave function scales as  $1/B^2$ . Since, the nonperturbative gluon rescattering kernels [47] do not allow for an analytical expression of the pion Boer-Mulders function, we proceed with its numerical computation. The standard deviation for  $\kappa$  is around 5%. Similarly, we apply a 5% uncertainty in the quark mass [69].

#### 4.2. Proton TMDs

For the proton TMDs, we utilize the light-front quark-diquark model constructed by the soft-wall AdS/QCD [71–74]. The T-even TMDs of the proton relevant to the structure functions, Eq. (4), can be expressed in terms of the LFWFs as follows:

$$f_{1,p}^q(x, k_\perp^2) = \frac{1}{16\pi^3} \left[ |\Psi_+^+(x, \vec{k}_\perp)|^2 + |\Psi_-^-(x, \vec{k}_\perp)|^2 \right], \quad (23)$$

$$h_{1,p}^q(x, k_\perp^2) = \frac{1}{16\pi^3} \left[ \Psi_+^{+\ast}(x, \vec{k}_\perp) \Psi_-^-(x, \vec{k}_\perp) \right], \quad (24)$$

$$h_{1,p}^{\perp q}(x, k_\perp^2) = \frac{1}{16\pi^3} \frac{2M}{k_\perp^2} \left[ k_\perp^r \Psi_-^{+\ast}(x, \vec{k}_\perp) \Psi_+^-(x, \vec{k}_\perp) \right], \quad (25)$$

$$h_{1T,p}^{\perp q}(x, k_\perp^2) = \frac{1}{16\pi^3} \frac{M^2}{k_1^2 - k_2^2} \left[ \Psi_-^{+*}(x, \vec{k}_\perp) \Psi_+^-(x, \vec{k}_\perp) + \Psi_+^{-*}(x, \vec{k}_\perp) \Psi_-^+(x, \vec{k}_\perp) \right], \quad (26)$$

where  $\Psi_{\lambda_q}^{\lambda_N}(x, \vec{k}_\perp)$  are the LFWFs with the proton helicities  $\lambda_N = \pm$  and for the quark  $\lambda_q = \pm$ ; plus and minus correspond to  $+\frac{1}{2}$  and  $-\frac{1}{2}$ , respectively and  $k_\perp^{r(l)} = k_1 \pm ik_2$ .

For the T-odd TMDs, the Sivers and Boer-Mulders functions, it is essential to consider the gauge link. Using the gluon rescattering kernel,  $G(x, |\vec{k}_\perp - \vec{k}'_\perp|)$ , and the LFWFs, they can be represented as,

$$f_{1T,p}^{\perp q}(x, k_\perp^2) = \frac{2M}{k_\perp^l} \int \frac{d^2 \vec{k}'_\perp}{16\pi^3} iG(x, |\vec{k}_\perp - \vec{k}'_\perp|) \times \sum_{\lambda_q} \left[ \Psi_{\lambda_q}^{+*}(x, \vec{k}'_\perp) \Psi_{\lambda_q}^-(x, \vec{k}_\perp) \right], \quad (27)$$

$$h_{1,p}^{\perp q}(x, k_\perp^2) = \frac{2M}{k_\perp^l} \int \frac{d^2 \vec{k}'_\perp}{16\pi^3} iG(x, |\vec{k}_\perp - \vec{k}'_\perp|) \times \sum_{\lambda_q, \lambda'_q} \left[ \Psi_{\lambda'_q}^{+*}(x, \vec{k}'_\perp) \Psi_{\lambda_q}^+(x, \vec{k}_\perp) \right]. \quad (28)$$

Using the proton LFWFs from the quark-diquark model [72–74], one can derive the analytical expressions for the quark TMDs by substituting them into the above Eqs. (23)–(28). The expressions for the T-even TMDs read as

$$f_{1,p}^q(x, k_\perp^2) = \frac{\log(1/x)}{\pi\kappa^2} \left( F_1^q(x) + \frac{k_\perp^2}{M^2} F_2^q(x) \right) \times \exp \left[ -\frac{k_\perp^2 \log(1/x)}{\kappa^2(1-x)^2} \right], \quad (29)$$

$$h_{1,p}^q(x, k_\perp^2) = \frac{\log(1/x)}{\pi\kappa^2} F_1^q(x) \exp \left[ -\frac{k_\perp^2 \log(1/x)}{\kappa^2(1-x)^2} \right], \quad (30)$$

$$h_{1L,p}^{\perp q}(x, k_\perp^2) = -\frac{2\log(1/x)}{\pi\kappa^2} F_3^q(x) \exp \left[ -\frac{k_\perp^2 \log(1/x)}{\kappa^2(1-x)^2} \right], \quad (31)$$

$$h_{1T,p}^{\perp q}(x, k_\perp^2) = -\frac{2\log(1/x)}{\pi\kappa^2} F_2^q(x) \exp \left[ -\frac{k_\perp^2 \log(1/x)}{\kappa^2(1-x)^2} \right], \quad (32)$$

where the parametrized functions  $F_i^q(x)$  are given by,

$$\begin{aligned} F_1^q(x) &= \left| N_q^{(1)} \right|^2 x^{2a_q^{(1)}} (1-x)^{2b_q^{(1)}-1}, \\ F_2^q(x) &= \left| N_q^{(2)} \right|^2 x^{2a_q^{(2)}-2} (1-x)^{2b_q^{(2)}-1}, \\ F_3^q(x) &= N_q^{(1)} N_q^{(2)} x^{a_q^{(1)}+a_q^{(2)}-1} (1-x)^{b_q^{(1)}+b_q^{(2)}-1}. \end{aligned} \quad (33)$$

The model parameters  $a_q^i$ ,  $b_q^i$  and the normalization constants  $N_q^i$ , along with the AdS/QCD scale parameter  $\kappa$  are determined by fitting the electromagnetic properties of the nucleons [73, 75]. This model has been widely used to study and effectively reproduce various noteworthy properties of the proton [38, 53, 72–77].

Using the perturbative gluon rescattering kernel, Eq. (16), the expressions for the Sivers and Boer-Mulders functions read as,

$$\begin{aligned} f_{1T,p}^{\perp q}(x, k_\perp^2) &\equiv h_{1(p)}^{\perp q}(x, k_\perp^2) = \frac{4}{\pi} C_F \alpha_s (1-x)^2 F_3^q(x) \frac{1}{k_\perp^2} \\ &\times \exp \left[ -\frac{k_\perp^2 \log(1/x)}{\kappa^2(1-x)^2} \right] \left( 1 - \exp \left[ \frac{k_\perp^2 \log(1/x)}{2\kappa^2(1-x)^2} \right] \right). \end{aligned} \quad (34)$$

In our scalar quark-diquark model, both the Sivers and Boer-Mulders TMDs for up and down quarks have the same sign, a distinct feature of this model as seen in prior study [32, 36, 40, 78]. Introducing the axial-vector diquark may alter these relations for the up and the down quarks [36, 39, 79, 80]. In a similar fashion to the pion's Boer-Mulders TMD, we conduct numerical computations for the proton's T-odd TMDs employing nonperturbative gluon rescattering kernels.

## 5. Numerical results

We analyze the single azimuthal transverse spin asymmetries in the polarized DY process within the kinematics of the COMPASS experiment, where the DY cross section for a proton target is predominantly influenced by contributions from the proton's  $u$ -quark and the pion's  $\bar{u}$ -quark TMDs [27],

$$0.05 < x_N < 0.4, \quad 0.05 < x_\pi < 0.9, \quad -0.3 < x_F < 1 \quad (35) \\ 4.3 \text{ GeV} < Q < 8.5 \text{ GeV}, \quad s = 357 \text{ GeV}^2.$$

We evolve the pion TMDs from the model scale  $Q_0^\pi \sim 0.316 \text{ GeV}$  [66, 69] to the scale  $Q_f \sim 6.4 \text{ GeV}$  relevant to the experimental data for the asymmetries following QCD evolution discussed in section 3. The proton TMDs are also evolved from the model scale of the quark-diquark model  $Q_0^p \sim 0.56 \text{ GeV}$  [38, 77] to the experimental scale.

Figure 1 presents the  $\sin(\phi_s)$  asymmetry, which is known as the Sivers asymmetry. This asymmetry arises from the convolution of the unpolarized parton distribution of the incoming pion beam and the Sivers function of the transversely polarized target proton, i.e.,  $A_{UT}^{\sin(\phi_s)} \propto f_{1,\pi}^q \otimes f_{1T,p}^{\perp q}$ . The perturbative and nonperturbative curves represent the asymmetries generated by using the perturbative and nonperturbative gluon rescattering kernels for the proton Sivers function. We compare our pure model results with recently reported COMPASS data [27, 28] and also with available theoretical predictions reported in Ref. [12], where the nonperturbative input for the pion TMD is taken from the light-front constituent quark model (LFCQM) [44] and the spectator model (SPM) [43], and the proton TMD is adopted from the LFCQM [83–85] and the SPM [34] as well as from the available Parametrization of TMDs extracted from the experimental data by Torino Collaboration [86] and JAM20 Collaboration [81].

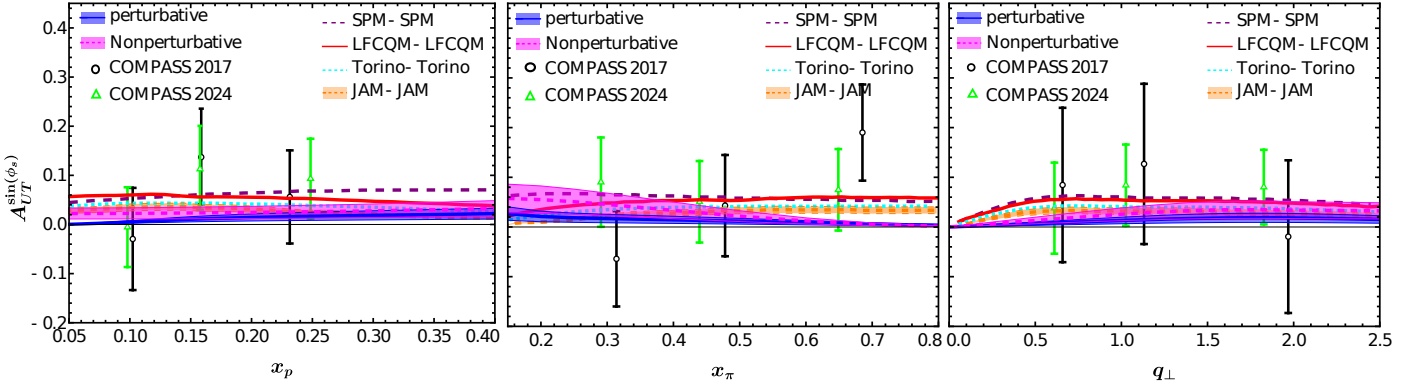


Figure 1:  $\sin(\phi_S)$  azimuthal asymmetry in pion-proton induced DY process. The panels from left to right show the variation of the azimuthal asymmetry with  $x_p$ ,  $x_\pi$ , and  $q_\perp$ , respectively. The black open circles and green up-triangles represent the COMPASS data [27, 28]. Our estimations (blue and magenta bands) are compared with the results obtained from pure model and hybrid calculations reported in Ref. [12]. The purple-dashed and solid-red lines show the pure model calculations from SPM [43] and LFCQM [44] models, while the orange band and cyan dashed lines represent the phenomenological computations from JAM [81] and Torino [82] collaborations, respectively.

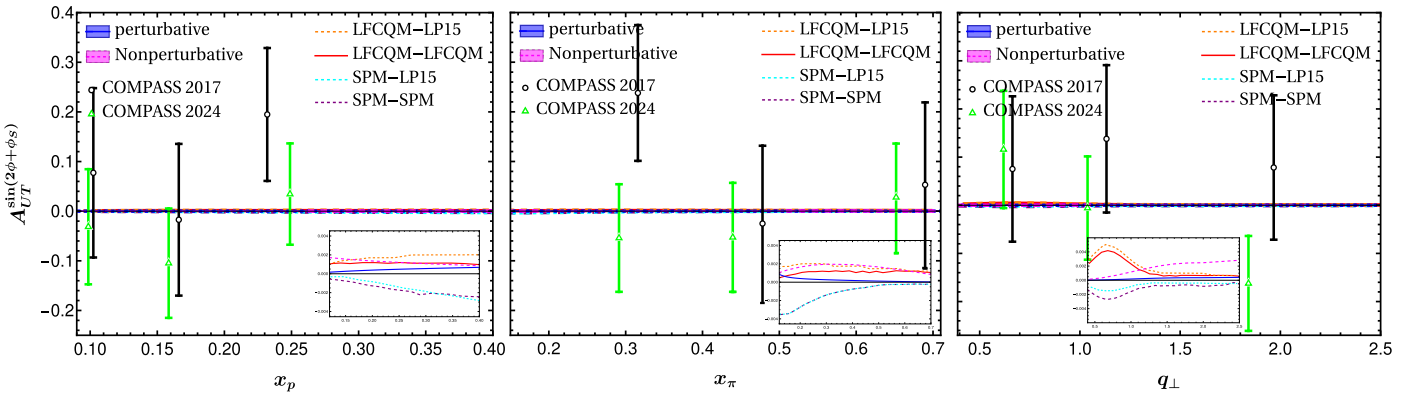


Figure 2:  $\sin(2\phi + \phi_S)$  azimuthal asymmetry in pion-proton induced DY process. The panels from left to right show the variation of the azimuthal asymmetry with  $x_p$ ,  $x_\pi$ , and  $q_\perp$ , respectively. The black open circles and green up-triangles represent the COMPASS data [27, 28]. Our estimations (blue and magenta bands) are compared with the results obtained from pure model and hybrid calculations reported in Ref. [12]. The orange and cyan lines represent the hybrid computations of SPM and LFCQM models with LP15 extractions of pretzelosity TMD [51], while the purple-dashed and solid red lines shows the pure model calculations from SPM [43] and LFCQM [44] models, respectively.

We observe that our model computations for the Sivers asymmetry are consistently positive across the entire range of COMPASS kinematics, which aligns well with both the COMPASS 2017 and COMPASS 2024 results [27, 28]. Disregarding the contribution from sea quarks, we can infer that  $A_{UT}^{\sin(\phi_S)} \propto f_{1T,p}^{\perp u} > 0$  as the unpolarized distribution of the pion's valence quarks is always positive [87]. This suggests that the  $u$ -quark Sivers function of the proton is positive in the DY process, whereas it is negative in the SIDIS process, a finding consistent with various theoretical analyses [36, 38, 39, 85] and phenomenological studies [22, 88–93]. The Sivers asymmetry is unique in that it can be fully described by both model predictions and available parametrizations like JAM20 [81] and Torino [82]. It serves as confirmation of the sign change of the Sivers function in both SIDIS (final state interactions) and DY (initial state interactions) processes observed in COMPASS [27, 28] and RHIC [94].

Figure 2 illustrates the  $\sin(2\phi + \phi_S)$  asymmetry, which is obtained by the convolution of pion Boer-Mulders function and the proton pretzelosity TMD, i.e.,  $A_{UT}^{\sin(2\phi + \phi_S)} \propto h_{1,\pi}^{\perp \bar{q}} \otimes h_{1T,p}^{\perp q}$ . We compare our model calculations with the available data [27, 28]. This asymmetry has been studied theoretically in SPM and LFCQM [43, 44] and also studied with LP15 extracted proton pretzelosity distribution [51] along with SPM and LFCQM. This asymmetry is notably smaller compared to others, primarily because the pretzelosity TMD has a much smaller magnitude than other TMDs. Additionally, this asymmetry is proportional to  $q_\perp^3$  for  $q_\perp \ll 1$  GeV, while the other asymmetries are proportional to  $q_\perp$ . Consequently, this asymmetry is the smallest among the leading-twist asymmetries in pion-nucleon DY, typically amounting to 1% or less numerically. To facilitate comparison with other model results, we provide insets indicating that the sign and magnitude of our asymmetry align with the SPM and LFCQM [12], while the sign is opposite for the LP15 fit of pretzelosity [51]. The

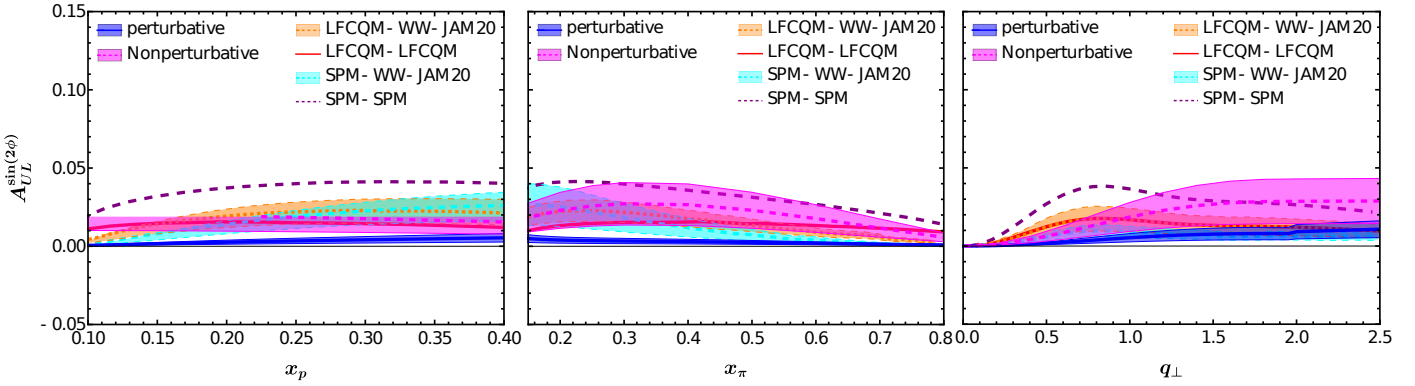


Figure 3:  $\sin(2\phi)$  azimuthal asymmetry in pion-proton induced DY process. The panels from left to right show the variation of the azimuthal asymmetry with  $x_p$ ,  $x_\pi$ , and  $q_\perp$ , respectively. Our estimations (blue and magenta bands) are compared with the results obtained from pure model and hybrid calculations reported in Ref. [12]. The orange and cyan bands represent the hybrid computations of LFCQM and SPM models with JAM20 fit of proton WW-type approximation of Kotzinian-Mulders function [95], while the purple-dashed and solid-red lines shows the pure model calculations from SPM [43] and LFCQM [44] models, respectively.

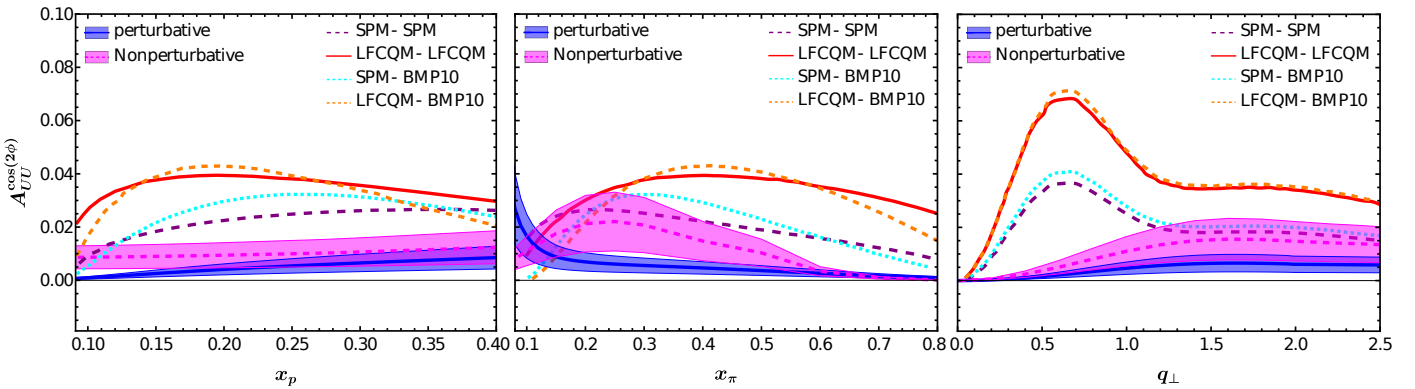


Figure 4:  $\cos(2\phi)$  azimuthal asymmetry in pion-proton induced DY process. The panels from left to right show the variation of the azimuthal asymmetry with  $x_p$ ,  $x_\pi$ , and  $q_\perp$ , respectively. Our estimations (blue and magenta bands) are compared with the results obtained from pure model and hybrid calculations reported in Ref. [12]. The purple-dashed and solid-red lines show the pure model calculations from SPM [43] and LFCQM [44] models, while the orange and cyan lines represent the hybrid computations of LFCQM and SPM models with BMP10 parametrization [96], respectively.

sign difference of pretzelosity distribution between model calculations and the first extraction from preliminary experimental data, suggest that the pion-induced DY process with a polarized proton opens a way to access the information on the pretzelosity distribution. Quantifying the pretzelosity TMD in DY and SIDIS presents inherent challenges. Nevertheless, the forthcoming high luminosity SIDIS experiments at JLab 12 GeV [97] and the prospective Electron-Ion Colliders [98, 99] provide a promising avenue for the feasible measurement of pretzelosity.

In Fig. 3, we present the  $\sin(2\phi)$  longitudinal single-spin asymmetry. This asymmetry is obtained from the convolution of T-odd pion Boer-Mulders function and the proton Kotzinian-Mulders function, i.e.,  $A_{UL}^{\sin(2\phi)} \propto -h_{1,\pi}^{\perp\bar{q}} \otimes h_{1L,p}^{\perp q}$ . We observe a positive distribution in our predicted asymmetry, indicating that the up quark Kotzinian-Mulders function is negative. This inference follows our earlier investigation [69], where we established the positivity of

the pion Boer-Mulders function for the up quark. We find that our results are compatible with the predictions yielding from both the pure-model (LFCQM-LFCQM and SPM-SPM) and the hybrid calculations (LFCQM-WW-JAM20 and SPM-WW-JAM20) [12]. This asymmetry remains unmeasurable in COMPASS as it necessitates longitudinal polarization of the proton target for observation. Nonetheless, there is potential for future exploration of this phenomenon through DY experiments employing doubly polarized protons or deuterons, potentially within the framework of the NICA experiment [100].

In Fig. 4, we show our predictions for the Boer-Mulders or  $\cos(2\phi)$  asymmetry in  $\pi^- p$  unpolarized Drell-Yan process. This asymmetry is computed from the convolution of pion Boer-Mulders function and the proton Boer-Mulders function, i.e.,  $A_{UU}^{\cos(2\phi)} \propto h_{1,\pi}^{\perp\bar{q}} \otimes h_{1,p}^{\perp q}$ . There is no experimental data from COMPASS for this asymmetry. However, a proposed strategy for analyzing this asymmetry has

been outlined in ref. [29]. We compare our predictions with pure models (SPM-SPM and LFCQM-LFCQM) as well as with hybrid calculations. In the hybrid calculations, the proton Boer-Mulders function is sourced from the BMP10 extraction [96], while the pion Boer-Mulders function is derived from both LFCQM [44] and SPM [43]. We note that the magnitude of our predicted asymmetry is slightly smaller when compared to that of other theoretical predictions. Note that this asymmetry has also been investigated in ref. [101], where pion distributions are based on a light-cone model, while the proton distribution is adopted from the BMP10 extraction. Analyzing the results presented in Fig. 4 allows for the determination of the sign of the proton Boer-Mulders function. The positive distribution of the  $\cos(2\phi)$  asymmetry across COMPASS kinematics leads to the inference that the proton Boer-Mulders function is positive in the DY process. This inference is supported by our prior discussion on the positivity of the pion Boer-Mulders function, from  $A_{UT}^{\sin(2\phi-\phi_s)}$  asymmetry [69]. Notably, this observation aligns with the sign change observed in the process-dependent T-odd distribution function, consistent with findings in SIDIS analyses [38–40].

In Figs. 1–4, we illustrate the distinctions between the asymmetries produced through the utilization of perturbative and nonperturbative gluon rescattering kernels for the T-odd pion and proton TMDs. Our findings reveal that both the perturbatively and nonperturbatively generated asymmetries align reasonably well with the available experimental data. Furthermore, it is noteworthy that the asymmetries generated nonperturbatively exhibit a slightly greater magnitude compared to those generated perturbatively.

## 6. Conclusion

We presented the azimuthal spin asymmetries, specifically  $\sin(\phi_s)$ ,  $\sin(2\phi + \phi_s)$ ,  $\sin(2\phi)$ , and  $\cos(2\phi)$  asymmetries, in the single transversely polarized  $\pi^- p$  Drell-Yan process within the TMD factorization formalism, focusing on the kinematics relevant to the COMPASS experiment. These asymmetries arise from the convolution of the TMDs of the pion beam and the proton target. We applied the holographic light-front QCD model to describe the pion, which leads to an excellent simultaneous depiction of a wide class of different and related pion observables. Additionally, we employed the widely used quark-diquark model constructed by the soft-wall AdS/QCD for the proton. Gluon rescattering plays a critical role in obtaining a non-zero pion's and proton's T-odd TMDs. We explored the utilization of a nonperturbative SU(3) gluon rescattering kernel, surpassing the conventional approximation of perturbative U(1) gluons.

After implementing the TMD evolution effect, we presented pure-model computations of the azimuthal asymmetries. Our analysis revealed that the asymmetries at

COMPASS can be qualitatively depicted (in terms of sign and magnitude) by the current analysis of the pion's TMDs within the holographic light-front QCD framework and the proton's TMDs within a light-front quark-diquark model motivated by the soft-wall AdS/QCD. With respect to interpreting the initial data from the pion-induced Drell-Yan process with polarized protons, we discerned a robust understanding. Our analysis led to the conclusion of positive T-odd TMDs for the up quark in the proton within the context of the Drell-Yan process, which is opposite to the sign observed in SIDIS analyses [23, 25, 26]. Based on the  $\sin(2\phi + \phi_s)$  asymmetry COMPASS data, no discernible trend is evident regarding the sign of the up quark's pretzelosity TMD. Nevertheless, we deduced a positive sign for this TMD, consistent with the predictions of the LFCQM and the SPM models, but contrasting with the LP15 fit of pretzelosity. Due to the relatively large statistical uncertainties in COMPASS data, clear trends are not discernible for any of the azimuthal spin asymmetries. Upcoming, more precise data from COMPASS and other experimental facilities will enable us to further solidify the picture. Our investigation has contributed to providing quantitative tests of the application of the holographic light-front QCD models to the description of the pion and the proton.

## Acknowledgement

The authors acknowledge fruitful discussions with B. Pasquini and D. Chakrabarti. The work of CM is supported by new faculty start up funding by the Institute of Modern Physics, Chinese Academy of Sciences, Grant No. E129952YR0. CM also thanks the Chinese Academy of Sciences Presidents International Fellowship Initiative for the support via Grants No. 2021PM0023.

## References

- [1] S. D. Drell, T.-M. Yan, Massive Lepton Pair Production in Hadron-Hadron Collisions at High-Energies, *Phys. Rev. Lett.* 25 (1970) 316–320, [Erratum: *Phys. Rev. Lett.* 25, 902 (1970)]. [doi:10.1103/PhysRevLett.25.316](https://doi.org/10.1103/PhysRevLett.25.316).
- [2] S. D. Drell, T.-M. Yan, Partons and their applications at high energies, *Annals of physics* 281 (1-2) (2000) 450–493.
- [3] J. Collins, Foundations of perturbative QCD, Vol. 32, Cambridge University Press, 2013.
- [4] R. Boussarie, et al., TMD Handbook (4 2023). [arXiv:2304.03302](https://arxiv.org/abs/2304.03302).
- [5] R. Angeles-Martinez, et al., Transverse Momentum Dependent (TMD) parton distribution functions: status and prospects, *Acta Phys. Polon. B* 46 (12) (2015) 2501–2534. [arXiv:1507.05267](https://arxiv.org/abs/1507.05267), [doi:10.5506/APhysPolB.46.2501](https://doi.org/10.5506/APhysPolB.46.2501).
- [6] R. N. Cahn, Azimuthal Dependence in Leptoproduction: A Simple Parton Model Calculation, *Phys. Lett. B* 78 (1978) 269–273. [doi:10.1016/0370-2693\(78\)90020-5](https://doi.org/10.1016/0370-2693(78)90020-5).
- [7] A. Bacchetta, M. Diehl, K. Goeke, A. Metz, P. J. Mulders, M. Schlegel, Semi-inclusive deep inelastic scattering at small transverse momentum, *JHEP* 02 (2007) 093. [arXiv:hep-ph/0611265](https://arxiv.org/abs/hep-ph/0611265), [doi:10.1088/1126-6708/2007/02/093](https://doi.org/10.1088/1126-6708/2007/02/093).

- [8] A. Bacchetta, V. Bertone, C. Bissolotti, G. Bozzi, M. Cerutti, F. Piacenza, M. Radici, A. Signori, Unpolarized transverse momentum distributions from a global fit of Drell-Yan and semi-inclusive deep-inelastic scattering data, JHEP 10 (2022) 127. [arXiv:2206.07598](https://arxiv.org/abs/2206.07598), doi:10.1007/JHEP10(2022)127.
- [9] R. D. Tangerman, P. J. Mulders, Intrinsic transverse momentum and the polarized Drell-Yan process, Phys. Rev. D 51 (1995) 3357–3372. [arXiv:hep-ph/9403227](https://arxiv.org/abs/hep-ph/9403227), doi:10.1103/PhysRevD.51.3357.
- [10] D. Boer, P. J. Mulders, Time reversal odd distribution functions in lepto-production, Phys. Rev. D 57 (1998) 5780–5786. [arXiv:hep-ph/9711485](https://arxiv.org/abs/hep-ph/9711485), doi:10.1103/PhysRevD.57.5780.
- [11] A. Bacchetta, V. Bertone, C. Bissolotti, G. Bozzi, F. Delcarro, F. Piacenza, M. Radici, Transverse-momentum-dependent parton distributions up to  $N^3LL$  from Drell-Yan data, JHEP 07 (2020) 117. [arXiv:1912.07550](https://arxiv.org/abs/1912.07550), doi:10.1007/JHEP07(2020)117.
- [12] S. Bastami, L. Gamberg, B. Parsamyan, B. Pasquini, A. Prokudin, P. Schweitzer, The Drell-Yan process with pions and polarized nucleons, JHEP 02 (2021) 166. [arXiv:2005.14322](https://arxiv.org/abs/2005.14322), doi:10.1007/JHEP02(2021)166.
- [13] D. W. Sivers, Single Spin Production Asymmetries from the Hard Scattering of Point-Like Constituents, Phys. Rev. D 41 (1990) 83. doi:10.1103/PhysRevD.41.83.
- [14] J. C. Collins, Leading twist single transverse-spin asymmetries: Drell-Yan and deep inelastic scattering, Phys. Lett. B 536 (2002) 43–48. [arXiv:hep-ph/0204004](https://arxiv.org/abs/hep-ph/0204004), doi:10.1016/S0370-2693(02)01819-1.
- [15] A. Airapetian, et al., Single-spin asymmetries in semi-inclusive deep-inelastic scattering on a transversely polarized hydrogen target, Phys. Rev. Lett. 94 (2005) 012002. [arXiv:hep-ex/0408013](https://arxiv.org/abs/hep-ex/0408013), doi:10.1103/PhysRevLett.94.012002.
- [16] A. Airapetian, et al., Observation of the Naive-T-odd Sivers Effect in Deep-Inelastic Scattering, Phys. Rev. Lett. 103 (2009) 152002. [arXiv:0906.3918](https://arxiv.org/abs/0906.3918), doi:10.1103/PhysRevLett.103.152002.
- [17] M. Alekseev, et al., Collins and Sivers asymmetries for pions and kaons in muon-deuteron DIS, Phys. Lett. B 673 (2009) 127–135. [arXiv:0802.2160](https://arxiv.org/abs/0802.2160), doi:10.1016/j.physletb.2009.01.060.
- [18] M. G. Alekseev, et al., Measurement of the Collins and Sivers asymmetries on transversely polarised protons, Phys. Lett. B 692 (2010) 240–246. [arXiv:1005.5609](https://arxiv.org/abs/1005.5609), doi:10.1016/j.physletb.2010.08.001.
- [19] C. Adolph, et al., II – Experimental investigation of transverse spin asymmetries in  $\mu$ -p SIDIS processes: Sivers asymmetries, Phys. Lett. B 717 (2012) 383–389. [arXiv:1205.5122](https://arxiv.org/abs/1205.5122), doi:10.1016/j.physletb.2012.09.056.
- [20] C. Adolph, et al., Sivers asymmetry extracted in SIDIS at the hard scales of the Drell-Yan process at COMPASS, Phys. Lett. B 770 (2017) 138–145. [arXiv:1609.07374](https://arxiv.org/abs/1609.07374), doi:10.1016/j.physletb.2017.04.042.
- [21] X. Qian, et al., Single Spin Asymmetries in Charged Pion Production from Semi-Inclusive Deep Inelastic Scattering on a Transversely Polarized  ${}^3\text{He}$  Target, Phys. Rev. Lett. 107 (2011) 072003. [arXiv:1106.0363](https://arxiv.org/abs/1106.0363), doi:10.1103/PhysRevLett.107.072003.
- [22] M. Anselmino, M. Boglione, U. D’Alesio, S. Melis, F. Murgia, A., Sivers effect in Drell-Yan processes, Phys. Rev. D 79 (2009) 054010. [arXiv:0901.3078](https://arxiv.org/abs/0901.3078), doi:10.1103/PhysRevD.79.054010.
- [23] Z.-B. Kang, J.-W. Qiu, Testing the Time-Reversal Modified Universality of the Sivers Function, Phys. Rev. Lett. 103 (2009) 172001. [arXiv:0903.3629](https://arxiv.org/abs/0903.3629), doi:10.1103/PhysRevLett.103.172001.
- [24] J.-C. Peng, J.-W. Qiu, Novel phenomenology of parton distributions from the Drell-Yan process, Prog. Part. Nucl. Phys. 76 (2014) 43–75. [arXiv:1401.0934](https://arxiv.org/abs/1401.0934), doi:10.1016/j.ppnp.2014.01.005.
- [25] S. J. Brodsky, D. S. Hwang, I. Schmidt, Final state interactions and single spin asymmetries in semiinclusive deep inelastic scattering, Phys. Lett. B 530 (2002) 99–107. [arXiv:hep-ph/0201296](https://arxiv.org/abs/hep-ph/0201296), doi:10.1016/S0370-2693(02)01320-5.
- [26] S. J. Brodsky, D. S. Hwang, I. Schmidt, Initial state interactions and single spin asymmetries in Drell-Yan processes, Nucl. Phys. B 642 (2002) 344–356. [arXiv:hep-ph/0206259](https://arxiv.org/abs/hep-ph/0206259), doi:10.1016/S0550-3213(02)00617-X.
- [27] M. Aghasyan, et al., First measurement of transverse-spin-dependent azimuthal asymmetries in the Drell-Yan process, Phys. Rev. Lett. 119 (11) (2017) 112002. [arXiv:1704.00488](https://arxiv.org/abs/1704.00488), doi:10.1103/PhysRevLett.119.112002.
- [28] G. D. Alexeev, et al., Final COMPASS results on the transverse-spin-dependent azimuthal asymmetries in the pion-induced Drell-Yan process (12 2023). [arXiv:2312.17379](https://arxiv.org/abs/2312.17379).
- [29] F. Gautheron, et al., COMPASS-II Proposal (5 2010).
- [30] L. Adamczyk, et al., Measurement of the transverse single-spin asymmetry in  $p^\uparrow + p \rightarrow W^\pm/Z^0$  at RHIC, Phys. Rev. Lett. 116 (13) (2016) 132301. [arXiv:1511.06003](https://arxiv.org/abs/1511.06003), doi:10.1103/PhysRevLett.116.132301.
- [31] D. Boer, Investigating the origins of transverse spin asymmetries at RHIC, Phys. Rev. D 60 (1999) 014012. [arXiv:hep-ph/9902255](https://arxiv.org/abs/hep-ph/9902255), doi:10.1103/PhysRevD.60.014012.
- [32] D. Boer, S. J. Brodsky, D. S. Hwang, Initial state interactions in the unpolarized Drell-Yan process, Phys. Rev. D 67 (2003) 054003. [arXiv:hep-ph/0211110](https://arxiv.org/abs/hep-ph/0211110), doi:10.1103/PhysRevD.67.054003.
- [33] G. R. Goldstein, L. Gamberg, Transversity and meson photo-production, in: 31st International Conference on High Energy Physics, 2002, pp. 452–454. [arXiv:hep-ph/0209085](https://arxiv.org/abs/hep-ph/0209085).
- [34] L. P. Gamberg, G. R. Goldstein, M. Schlegel, Transverse Quark Spin Effects and the Flavor Dependence of the Boer-Mulders Function, Phys. Rev. D 77 (2008) 094016. [arXiv:0708.0324](https://arxiv.org/abs/0708.0324), doi:10.1103/PhysRevD.77.094016.
- [35] M. Burkardt, B. Hannafous, Are all Boer-Mulders functions alike?, Phys. Lett. B 658 (2008) 130–137. [arXiv:0705.1573](https://arxiv.org/abs/0705.1573), doi:10.1016/j.physletb.2007.09.064.
- [36] A. Bacchetta, F. Conti, M. Radici, Transverse-momentum distributions in a diquark spectator model, Phys. Rev. D 78 (2008) 074010. [arXiv:0807.0323](https://arxiv.org/abs/0807.0323), doi:10.1103/PhysRevD.78.074010.
- [37] S. Meissner, A. Metz, K. Goeke, Relations between generalized and transverse momentum dependent parton distributions, Phys. Rev. D 76 (2007) 034002. [arXiv:hep-ph/0703176](https://arxiv.org/abs/hep-ph/0703176), doi:10.1103/PhysRevD.76.034002.
- [38] B. Gurjar, D. Chakrabarti, C. Mondal, Sivers and Boer-Mulders TMDs of the proton in a light-front quark-diquark model, Phys. Rev. D 106 (11) (2022) 114027. [arXiv:2207.11527](https://arxiv.org/abs/2207.11527), doi:10.1103/PhysRevD.106.114027.
- [39] T. Maji, D. Chakrabarti, A. Mukherjee, Sivers and  $\cos 2\phi$  asymmetries in semi-inclusive deep inelastic scattering in light-front holographic model, Phys. Rev. D 97 (1) (2018) 014016. [arXiv:1711.02930](https://arxiv.org/abs/1711.02930), doi:10.1103/PhysRevD.97.014016.
- [40] V. E. Lyubovitskij, I. Schmidt, S. J. Brodsky, Predictions for the Sivers single-spin asymmetry from holographic QCD, Phys. Rev. D 105 (11) (2022) 114032. [arXiv:2205.08986](https://arxiv.org/abs/2205.08986), doi:10.1103/PhysRevD.105.114032.
- [41] A. Courtoy, S. Scopetta, V. Vento, Analyzing the Boer-Mulders function within different quark models, Phys. Rev. D 80 (2009) 074032. [arXiv:0909.1404](https://arxiv.org/abs/0909.1404), doi:10.1103/PhysRevD.80.074032.
- [42] B. Pasquini, F. Yuan, Sivers and Boer-Mulders functions in Light-Cone Quark Models, Phys. Rev. D 81 (2010) 114013. [arXiv:1001.5398](https://arxiv.org/abs/1001.5398), doi:10.1103/PhysRevD.81.114013.
- [43] L. Gamberg, M. Schlegel, Final state interactions and the transverse structure of the pion using non-perturbative eikonal methods, Phys. Lett. B 685 (2010) 95–103. [arXiv:0911.1964](https://arxiv.org/abs/0911.1964), doi:10.1016/j.physletb.2009.12.067.
- [44] B. Pasquini, P. Schweitzer, Pion transverse momentum dependent parton distributions in a light-front constituent approach, and the Boer-Mulders effect in the pion-induced Drell-Yan process, Phys. Rev. D 90 (1) (2014) 014050. [arXiv:1406.2056](https://arxiv.org/abs/1406.2056), doi:10.1103/PhysRevD.90.014050.
- [45] Z. Wang, X. Wang, Z. Lu, Boer-Mulders function of pion me-

- son and  $q_T$ -weighted  $\cos 2\phi$  asymmetry in the unpolarized  $\pi^- p$  Drell-Yan at COMPASS, Phys. Rev. D 95 (9) (2017) 094004. [arXiv:1702.03637](#), [doi:10.1103/PhysRevD.95.094004](#).
- [46] Z. Lu, B.-Q. Ma, J. Zhu, Boer-Mulders function of the pion in the MIT bag model, Phys. Rev. D 86 (2012) 094023. [arXiv:1211.1745](#), [doi:10.1103/PhysRevD.86.094023](#).
- [47] M. Ahmady, C. Mondal, R. Sandapen, Predicting the light-front holographic TMDs of the pion, Phys. Rev. D 100 (5) (2019) 054005. [arXiv:1907.06561](#), [doi:10.1103/PhysRevD.100.054005](#).
- [48] W. Kou, C. Shi, X. Chen, W. Jia, Transverse momentum dependent parton distributions of pion at leading twist, Phys. Rev. D 108 (3) (2023) 036021. [arXiv:2304.09814](#), [doi:10.1103/PhysRevD.108.036021](#).
- [49] S. Noguera, S. Scopetta, Pion transverse momentum dependent parton distributions in the Nambu and Jona-Lasinio model, JHEP 11 (2015) 102. [arXiv:1508.01061](#), [doi:10.1007/JHEP11\(2015\)102](#).
- [50] M. Engelhardt, P. Hägler, B. Musch, J. Negele, A. Schäfer, Lattice QCD study of the Boer-Mulders effect in a pion, Phys. Rev. D 93 (5) (2016) 054501. [arXiv:1506.07826](#), [doi:10.1103/PhysRevD.93.054501](#).
- [51] C. Lefkay, A. Prokudin, Extraction of the distribution function  $h_{1T}^\perp$  from experimental data, Phys. Rev. D 91 (3) (2015) 034010. [arXiv:1411.0580](#), [doi:10.1103/PhysRevD.91.034010](#).
- [52] J. C. Collins, D. E. Soper, G. F. Sterman, Transverse Momentum Distribution in Drell-Yan Pair and W and Z Boson Production, Nucl. Phys. B 250 (1985) 199–224. [doi:10.1016/0550-3213\(85\)90479-1](#).
- [53] T. Maji, C. Mondal, D. Chakrabarti, O. V. Teryaev, Relating transverse structure of various parton distributions, JHEP 01 (2016) 165. [arXiv:1506.04560](#), [doi:10.1007/JHEP01\(2016\)165](#).
- [54] J. Collins, T. Rogers, Understanding the large-distance behavior of transverse-momentum-dependent parton densities and the Collins-Soper evolution kernel, Phys. Rev. D 91 (7) (2015) 074020. [arXiv:1412.3820](#), [doi:10.1103/PhysRevD.91.074020](#).
- [55] S. Arnold, A. Metz, M. Schlegel, Dilepton production from polarized hadron hadron collisions, Phys. Rev. D 79 (2009) 034005. [arXiv:0809.2262](#), [doi:10.1103/PhysRevD.79.034005](#).
- [56] J.-C. Peng, D. Boer, W.-C. Chang, R. E. McClellan, O. Teryaev, On the rotational invariance and non-invariance of lepton angular distributions in Drell-Yan and quarkonium production, Phys. Lett. B 789 (2019) 356–359. [arXiv:1808.04398](#), [doi:10.1016/j.physletb.2018.11.061](#).
- [57] S. M. Aybat, T. C. Rogers, TMD Parton Distribution and Fragmentation Functions with QCD Evolution, Phys. Rev. D 83 (2011) 114042. [arXiv:1101.5057](#), [doi:10.1103/PhysRevD.83.114042](#).
- [58] A. Bacchetta, G. Bozzi, M. G. Echevarria, C. Pisano, A. Prokudin, M. Radici, Azimuthal asymmetries in unpolarized SIDIS and Drell-Yan processes: a case study towards TMD factorization at subleading twist, Phys. Lett. B 797 (2019) 134850. [arXiv:1906.07037](#), [doi:10.1016/j.physletb.2019.134850](#).
- [59] P. Sun, J. Isaacson, C. P. Yuan, F. Yuan, Nonperturbative functions for SIDIS and Drell-Yan processes, Int. J. Mod. Phys. A 33 (11) (2018) 1841006. [arXiv:1406.3073](#), [doi:10.1142/S0217751X18410063](#).
- [60] S. M. Aybat, J. C. Collins, J.-W. Qiu, T. C. Rogers, The QCD Evolution of the Sivers Function, Phys. Rev. D 85 (2012) 034043. [arXiv:1110.6428](#), [doi:10.1103/PhysRevD.85.034043](#).
- [61] M. G. Echevarria, A. Idilbi, Z.-B. Kang, I. Vitev, QCD Evolution of the Sivers Asymmetry, Phys. Rev. D 89 (2014) 074013. [arXiv:1401.5078](#), [doi:10.1103/PhysRevD.89.074013](#).
- [62] T. Altonen, et al., Transverse momentum cross section of  $e^+e^-$  pairs in the  $Z$ -boson region from  $p\bar{p}$  collisions at  $\sqrt{s} = 1.96$  TeV, Phys. Rev. D 86 (2012) 052010. [arXiv:1207.7138](#), [doi:10.1103/PhysRevD.86.052010](#).
- [63] V. M. Abazov, et al., Measurement of the shape of the boson transverse momentum distribution in  $p\bar{p} \rightarrow Z/\gamma^* \rightarrow e^+e^- + X$  events produced at  $\sqrt{s}=1.96$ -TeV, Phys. Rev. Lett. 100 (2008) 102002. [arXiv:0712.0803](#), [doi:10.1103/PhysRevLett.100.102002](#).
- [64] J. S. Conway, et al., Experimental Study of Muon Pairs Produced by 252-GeV Pions on Tungsten, Phys. Rev. D 39 (1989) 92–122. [doi:10.1103/PhysRevD.39.92](#).
- [65] S. J. Brodsky, G. F. de Teramond, H. G. Dosch, J. Erlich, Light-Front Holographic QCD and Emerging Confinement, Phys. Rept. 584 (2015) 1–105. [arXiv:1407.8131](#), [doi:10.1016/j.physrep.2015.05.001](#).
- [66] M. Ahmady, C. Mondal, R. Sandapen, Dynamical spin effects in the holographic light-front wavefunctions of light pseudoscalar mesons, Phys. Rev. D 98 (3) (2018) 034010. [arXiv:1805.08911](#), [doi:10.1103/PhysRevD.98.034010](#).
- [67] S. J. Brodsky, G. F. de Téramond, H. G. Dosch, C. Lorcé, Universal Effective Hadron Dynamics from Superconformal Algebra, Phys. Lett. B 759 (2016) 171–177. [arXiv:1604.06746](#), [doi:10.1016/j.physletb.2016.05.068](#).
- [68] M. Ahmady, F. Chishtie, R. Sandapen, Spin effects in the pion holographic light-front wavefunction, Phys. Rev. D 95 (7) (2017) 074008. [arXiv:1609.07024](#), [doi:10.1103/PhysRevD.95.074008](#).
- [69] B. Gurjar, C. Mondal, Predicting  $\sin(2\phi-\phi_S)$  azimuthal asymmetry in pion-proton induced Drell-Yan process using holographic light-front QCD, Phys. Rev. D 109 (1) (2024) 014038. [arXiv:2308.14528](#), [doi:10.1103/PhysRevD.109.014038](#).
- [70] M. Ahmady, S. Kaur, C. Mondal, R. Sandapen, Light-front holographic radiative transition form factors for light mesons, Phys. Rev. D 102 (3) (2020) 034021. [arXiv:2006.07675](#), [doi:10.1103/PhysRevD.102.034021](#).
- [71] T. Gutsche, V. E. Lyubovitskij, I. Schmidt, A. Vega, Light-front quark model consistent with Drell-Yan-West duality and quark counting rules, Phys. Rev. D 89 (5) (2014) 054033, [Erratum: Phys. Rev. D 92, 019902 (2015)]. [arXiv:1306.0366](#), [doi:10.1103/PhysRevD.89.054033](#).
- [72] D. Chakrabarti, C. Mondal, A. Mukherjee, Gravitational form factors and transverse spin sum rule in a light front quark-diquark model in AdS/QCD, Phys. Rev. D 91 (11) (2015) 114026. [arXiv:1505.02013](#), [doi:10.1103/PhysRevD.91.114026](#).
- [73] D. Chakrabarti, C. Mondal, Chiral-odd generalized parton distributions for proton in a light-front quark-diquark model, Phys. Rev. D 92 (7) (2015) 074012. [arXiv:1509.00598](#), [doi:10.1103/PhysRevD.92.074012](#).
- [74] D. Chakrabarti, T. Maji, C. Mondal, A. Mukherjee, Wigner distributions and orbital angular momentum of a proton, Eur. Phys. J. C 76 (7) (2016) 409. [arXiv:1601.03217](#), [doi:10.1140/epjc/s10052-016-4258-7](#).
- [75] C. Mondal, D. Chakrabarti, A Comparative Study of Nucleon Structure in Light-Front Quark Models in AdS/QCD, Few Body Syst. 57 (8) (2016) 723–728. [arXiv:1601.01252](#), [doi:10.1007/s00601-016-1044-x](#).
- [76] C. Mondal, Helicity-dependent generalized parton distributions for nonzero skewness, Eur. Phys. J. C 77 (9) (2017) 640. [arXiv:1709.06877](#), [doi:10.1140/epjc/s10052-017-5203-0](#).
- [77] P. Choudhary, B. Gurjar, D. Chakrabarti, A. Mukherjee, Gravitational form factors and mechanical properties of the proton: Connections between distributions in 2D and 3D, Phys. Rev. D 106 (7) (2022) 076004. [arXiv:2206.12206](#), [doi:10.1103/PhysRevD.106.076004](#).
- [78] D. S. Hwang, Light-Cone Wavefunction Representations of Sivers and Boer-Mulders Distribution Functions, J. Korean Phys. Soc. 62 (2013) 581–590. [arXiv:1003.0867](#), [doi:10.3938/jkps.62.581](#).
- [79] J. R. Ellis, D. S. Hwang, A. Kotzinian, Sivers Asymmetries for Inclusive Pion and Kaon Production in Deep-Inelastic Scattering, Phys. Rev. D 80 (2009) 074033. [arXiv:0808.1567](#), [doi:10.1103/PhysRevD.80.074033](#).
- [80] B. Gurjar, D. Chakrabarti, P. Choudhary, A. Mukherjee, P. Talukdar, Relations between generalized parton distributions and transverse momentum dependent parton distribu-

- tions, Phys. Rev. D 104 (7) (2021) 076028. [arXiv:2107.02216](#), doi:[10.1103/PhysRevD.104.076028](#).
- [81] J. Cammarota, L. Gamberg, Z.-B. Kang, J. A. Miller, D. Pitonyak, A. Prokudin, T. C. Rogers, N. Sato, Origin of single transverse-spin asymmetries in high-energy collisions, Phys. Rev. D 102 (5) (2020) 054002. [arXiv:2002.08384](#), doi:[10.1103/PhysRevD.102.054002](#).
- [82] M. Anselmino, M. Boglione, U. D'Alesio, S. Melis, F. Murgia, A. Prokudin, Sivers Distribution Functions and the Latest SIDIS Data, DIS 2011 (7 2011). [arXiv:1107.4446](#).
- [83] B. Pasquini, S. Cazzaniga, S. Boffi, Transverse momentum dependent parton distributions in a light-cone quark model, Phys. Rev. D 78 (2008) 034025. [arXiv:0806.2298](#), doi:[10.1103/PhysRevD.78.034025](#).
- [84] S. Boffi, A. V. Efremov, B. Pasquini, P. Schweitzer, Azimuthal spin asymmetries in light-cone constituent quark models, Phys. Rev. D 79 (2009) 094012. [arXiv:0903.1271](#), doi:[10.1103/PhysRevD.79.094012](#).
- [85] B. Pasquini, P. Schweitzer, Naive time-reversal odd phenomena in semi-inclusive deep-inelastic scattering from light-cone constituent quark models, Phys. Rev. D 83 (2011) 114044. [arXiv:1103.5977](#), doi:[10.1103/PhysRevD.83.114044](#).
- [86] M. Anselmino, M. Boglione, U. D'Alesio, S. Melis, F. Murgia, A. Prokudin, Simultaneous extraction of transversity and Collins functions from new SIDIS and e+e- data, Phys. Rev. D 87 (2013) 094019. [arXiv:1303.3822](#), doi:[10.1103/PhysRevD.87.094019](#).
- [87] M. Cerutti, L. Rossi, S. Venturini, A. Bacchetta, V. Bertone, C. Bissolotti, M. Radici, Extraction of pion transverse momentum distributions from Drell-Yan data, Phys. Rev. D 107 (1) (2023) 014014. [arXiv:2210.01733](#), doi:[10.1103/PhysRevD.107.014014](#).
- [88] A. V. Efremov, K. Goeke, S. Menzel, A. Metz, P. Schweitzer, Sivers effect in semi-inclusive DIS and in the Drell-Yan process, Phys. Lett. B 612 (2005) 233–244. [arXiv:hep-ph/0412353](#), doi:[10.1016/j.physletb.2005.03.010](#).
- [89] M. Anselmino, M. Boglione, U. D'Alesio, A. Kotzinian, S. Melis, F. Murgia, A. Prokudin, C. Turk, Sivers Effect for Pion and Kaon Production in Semi-Inclusive Deep Inelastic Scattering, Eur. Phys. J. A 39 (2009) 89–100. [arXiv:0805.2677](#), doi:[10.1140/epja/i2008-10697-y](#).
- [90] M. Anselmino, M. Boglione, U. D'Alesio, A. Kotzinian, F. Murgia, A. Prokudin, Extracting the Sivers function from polarized SIDIS data and making predictions, Phys. Rev. D 72 (2005) 094007, [Erratum: Phys.Rev.D 72, 099903 (2005)]. [arXiv:hep-ph/0507181](#), doi:[10.1103/PhysRevD.72.094007](#).
- [91] I. P. Fernando, D. Keller, Extraction of the Sivers function with deep neural networks, Phys. Rev. D 108 (5) (2023) 054007. [arXiv:2304.14328](#), doi:[10.1103/PhysRevD.108.054007](#).
- [92] M. Bury, A. Prokudin, A. Vladimirov, Extraction of the Sivers function from SIDIS, Drell-Yan, and  $W^\pm/Z$  boson production data with TMD evolution, JHEP 05 (2021) 151. [arXiv:2103.03270](#), doi:[10.1007/JHEP05\(2021\)151](#).
- [93] M. Bury, A. Prokudin, A. Vladimirov, Extraction of the Sivers Function from SIDIS, Drell-Yan, and  $W^\pm/Z$  Data at Next-to-Next-to-Next-to Leading Order, Phys. Rev. Lett. 126 (11) (2021) 112002. [arXiv:2012.05135](#), doi:[10.1103/PhysRevLett.126.112002](#).
- [94] E.-C. Aschenauer, et al., The RHIC SPIN Program: Achievements and Future Opportunities (1 2015). [arXiv:1501.01220](#).
- [95] S. Bastami, et al., Semi-Inclusive Deep Inelastic Scattering in Wandzura-Wilczek-type approximation, JHEP 06 (2019) 007. [arXiv:1807.10606](#), doi:[10.1007/JHEP06\(2019\)007](#).
- [96] V. Barone, S. Melis, A. Prokudin, The Boer-Mulders effect in unpolarized SIDIS: An Analysis of the COMPASS and HERMES data on the  $\cos 2\phi$  asymmetry, Phys. Rev. D 81 (2010) 114026. [arXiv:0912.5194](#), doi:[10.1103/PhysRevD.81.114026](#).
- [97] J. Dudek, et al., Physics Opportunities with the 12 GeV Upgrade at Jefferson Lab, Eur. Phys. J. A 48 (2012) 187. [arXiv:1208.1244](#), doi:[10.1140/epja/i2012-12187-1](#).
- [98] R. Abdul Khalek, et al., Science Requirements and Detector Concepts for the Electron-Ion Collider: EIC Yellow Report, Nucl. Phys. A 1026 (2022) 122447. [arXiv:2103.05419](#), doi:[10.1016/j.nuclphysa.2022.122447](#).
- [99] D. P. Anderle, et al., Electron-ion collider in China, Front. Phys. (Beijing) 16 (6) (2021) 64701. [arXiv:2102.09222](#), doi:[10.1007/s11467-021-1062-0](#).
- [100] I. A. Savin, et al., Spin Physics Experiments at NICA-SPD with polarized proton and deuteron beams, EPJ Web Conf. 85 (2015) 02039. [arXiv:1408.3959](#), doi:[10.1051/epjconf/20158502039](#).
- [101] X. Wang, W. Mao, Z. Lu, Boer-Mulders effect in the unpolarized pion induced Drell-Yan process at COMPASS within TMD factorization, Eur. Phys. J. C 78 (8) (2018) 643. [arXiv:1805.03017](#), doi:[10.1140/epjc/s10052-018-6114-4](#).